Shear-improved Smagorinsky model for large-eddy simulation of wall-bounded turbulent flows

Emmanuel Lévêque, F. Toschi, Liang Shao, Jean-Pierre Bertoglio

▶ To cite this version:

Shear-improved Smagorinsky model for large-eddy simulation of wall-bounded turbulent flows

By E. LÉVÊQUE[1], F. TOSCHI[2,3], L. SHAO[4]
AND J.-P. BERTOGLIO[4]

[1]Laboratoire de Physique, CNRS, Université de Lyon, École normale supérieure de Lyon, France

[2]Istituto per le Applicazioni del Calcolo, CNR, Viale del Policlinico 137, I-00161, Roma, Italy

[3]INFN, Sezione di Ferrara, Via G. Saragat 1, I-44100 Ferrara, Italy

[4]Laboratoire de Mécanique des Fluides et d'Acoustique, CNRS, Université de Lyon,
École centrale de Lyon, Université Lyon 1, INSA de Lyon, France

A shear-improved Smagorinsky model is introduced based on results concerning mean-shear effects in wall-bounded turbulence. The Smagorinsky eddy-viscosity is modified as $\nu_T = (C_s \Delta)^2(|\bar{S}| - |\langle \bar{S} \rangle|)$: the magnitude of the mean shear $|\langle \bar{S} \rangle|$ is subtracted from the magnitude of the instantaneous resolved rate-of-strain tensor $|\bar{S}|$; C_S is the standard Smagorinsky constant and Δ denotes the grid spacing. This subgrid-scale model is tested in large-eddy simulations of plane-channel flows at Reynolds numbers $Re_\tau = 395$ and $Re_\tau = 590$. First comparisons with the dynamic Smagorinsky model and direct numerical simulations for mean velocity, turbulent kinetic energy and Reynolds stress profiles, are shown to be extremely satisfactory. The proposed model, in addition to being physically sound and consistent with the scale-by-scale energy budget of locally homogeneous shear turbulence, has a low computational cost and possesses a high potential for generalization to complex non-homogeneous turbulent flows.

1. Introduction

The prohibitive cost of direct numerical simulations (DNS) of turbulent engineering flows motivate the development of simplified models, requiring less computation, but still relevant (to some degree) for reproducing the large-scale dynamics (Deardorff 1970; Lesieur & Metais 1996; Piomelli 1999; Sagaut 2001). Under these circumstances, the modelling of turbulent flows near a solid boundary is of special interest. A boundary affects the kinetics of the flow through different mechanisms. The most prominent is that related to the mean shear, which is extreme at the boundary and responsible for the production of streamwise vortices and streaky structures, which eventually detach and sustain turbulence in the bulk (Perot & Moin 1995). Thus, it is thought that understanding how the mean shear impacts on fluid motions is a key to improving the capabilities of numerical models. In the present work, we present a subgrid-scale model of turbulence which may be viewed as an improvement over the popular Smagorinsky model, in the presence of a mean shear. Our model originates from theoretical findings concerning shear effects in wall-bounded turbulence (Toschi, Lévêque & Ruiz-Chavarria 2000). Quite simply, we argue that the magnitude of

the mean shear should be subtracted from the magnitude of the resolved strain-rate tensor in the definition of the eddy-viscosity. As will be discussed later, this improvement accounts for the non-isotropic nature of the flow near the boundary and, at the same time, allows us to recover the standard Smagorinsky model in regions of (locally) homogeneous and isotropic turbulence. The general framework of the so-called large-eddy simulation (LES) of turbulent flows is now briefly recalled.

Roughly speaking, large-scale motions transport most of the kinetic energy of the flow. Their strength make them the most efficient carriers of conserved quantities (momentum, heat, mass, etc.). On the contrary, small-scale motions are primarily responsible for the dissipation, but they are weaker and contribute little to transport. From mechanical aspects, the large-scale (energy-carrying) dynamics are thus of particular importance and the costly computation of small-scale dynamics should be avoided. Furthermore, while large-scale motions are strongly dependent on the external flow conditions, small-scale motions are expected to behave more universally. Hence, there is a hope that numerical modelling can be feasible and/or require few adjustments when applied to various flows.

In LES, only the large-scale components of flow variables are explicitly integrated in time, and interactions with the unresolved small-scale components are modelled. A spatial filtering is conceptually introduced as $\overline{\phi}(\boldsymbol{x}, t) = \int \phi(\boldsymbol{x}', t) G_\Delta(\boldsymbol{x} - \boldsymbol{x}') \, \mathrm{d}\boldsymbol{x}'$, where the filter width Δ fixes the size of the smallest scales of variation retained in the flow variable $\phi(\boldsymbol{x}, t)$ (Leonard 1974). In practice, Δ is chosen much larger than the spatial cutoff scale of $\phi(\boldsymbol{x}, t)$, i.e. the dissipative scale of turbulence, so that $\overline{\phi}(\boldsymbol{x}, t)$ may be properly considered as the large-scale component of $\phi(\boldsymbol{x}, t)$. Applying the previous filtering procedure to the Navier–Stokes equations (and neglecting here non-commutation errors, Ghosal & Moin 1995, for the sake of simplicity) yields

$$\frac{\partial \overline{u}_i}{\partial t} + \overline{u}_j \frac{\partial \overline{u}_i}{\partial x_j} + \frac{\partial \tau_{ij}}{\partial x_j} = -\frac{\partial \overline{p}}{\partial x_i} + \nu \frac{\partial^2 \overline{u}_i}{\partial x_k \partial x_k} \quad \text{with} \quad \frac{\partial \overline{u}_i}{\partial x_i} = 0, \tag{1.1}$$

where $\overline{u}_i(\boldsymbol{x}, t)$ and $\overline{p}(\boldsymbol{x}, t)$ represent the large-scale velocity and pressure, and ν is the kinematic viscosity of the fluid. The equations (1.1) are amenable to numerical discretization with a grid spacing comparable to Δ since $\overline{\boldsymbol{u}}(\boldsymbol{x}, t)$ varies smoothly over Δ. $\tau_{ij}(\boldsymbol{x}, t) \equiv \overline{u_i(\boldsymbol{x}, t) u_j(\boldsymbol{x}, t)} - \overline{u}_i(\boldsymbol{x}, t) \overline{u}_j(\boldsymbol{x}, t)$ is named the subgrid-scale (SGS) stress tensor and encompasses all interactions between the grid-scale and the (unresolved) subgrid-scale component of $\boldsymbol{u}(\boldsymbol{x}, t)$. In LES, $\tau_{ij}(\boldsymbol{x}, t)$ must be expressed in terms of the grid-scale velocity field $\overline{\boldsymbol{u}}(\boldsymbol{x}, t)$ only, which is the difficult problem (Lesieur 1997). Eddy-viscosity models parameterize the SGS stress tensor as

$$\tau_{ij} - \tfrac{1}{3} \delta_{ij} \tau_{kk} = -2\nu_T \overline{S}_{ij} \quad \text{where} \quad \overline{S}_{ij}(\boldsymbol{x}, t) \equiv \frac{1}{2} \left(\frac{\partial \overline{u}_i}{\partial x_j}(\boldsymbol{x}, t) + \frac{\partial \overline{u}_j}{\partial x_i}(\boldsymbol{x}, t) \right), \tag{1.2}$$

where $\nu_T(\boldsymbol{x}, t)$ is the scalar eddy-viscosity and $\overline{S}_{ij}$ is the resolved rate-of-strain tensor. This empirical modelization is rooted in the idea that SGS motions are primarily responsible for a diffusive transport of momentum from the rapid to the slow grid-scale flow regions. The theoretical basis for the use of an eddy-viscosity is rather insecure; however, it appears to be workable in practice (as advocated by Kraichnan 1976); $\nu_T(\boldsymbol{x}, t)$ is then primarily designed to ensure the correct mean drain of kinetic energy from the grid-scale flow to the SGS motions: $-\langle \tau_{ij} \overline{S}_{ij} \rangle$ from (1.1). Another important feature is that $\nu_T(\boldsymbol{x}, t)$ should vanish in laminar-flow regions, e.g. in the viscous sublayer near the boundary (Moin & Kim 1982). Accordingly, our main concern was to determine an eddy-viscosity $\nu_T(\boldsymbol{x}, t)$ that would take into account

mean-shear effects in the transfer of energy to the SGS motions (without any sort of dynamical adjustment) and naturally decrease to zero at the boundary (without using any *ad hoc* damping function).

In §2, the advantages and drawbacks of the Smagorinsky model, which is used as our baseline model, are recalled. The necessity for a model that can achieve a satisfactory compromise between accuracy and manageability is identified. A shear-improved Smagorinsky model is introduced within the classical picture of shear turbulence. In §3, we present results from LES of turbulent plane-channel flows at $Re_\tau = 395$ and $Re_\tau = 590$. Comparisons are carried out with the dynamic Smagorinsky model and DNS. Discussion and perspectives follow in §4.

2. A shear-improved Smagorinsky model

2.1. *Our baseline model: the Smagorinsky model*

The Smagorinsky model (Smagorinsky 1963) is certainly the simplest and most commonly used eddy-viscosity model (Pope 2000, for a comprehensive description). The prescription for ν_T is $\nu_T(\boldsymbol{x}, t) = (C_s\Delta)^2|\bar{S}(\boldsymbol{x}, t)|$, where $|\bar{S}| \equiv (2\bar{S}_{ij}\bar{S}_{ij})^{1/2}$ represents the magnitude of the resolved rate-of-strain and C_s is a non-dimensional coefficient called the Smagorinsky constant. The major merits of the Smagorinsky model are its manageability, its computational stability and the simplicity of its formulation (involving only one adjusted parameter). All this makes it a valuable tool for engineering applications (Rogallo & Moin 1984). However, while this model is found to give acceptable results in LES of homogeneous and isotropic turbulence, with $C_s \approx 0.17$ according to Lilly (1967), it is too dissipative with respect to the resolved motions in the near-wall region because of an excessive eddy-viscosity arising from the mean shear (Moin & Kim 1982). The eddy-viscosity predicted by Smagorinsky is non-zero in laminar-flow regions; the model introduces spurious dissipation which damps the growth of small perturbations and thus restrains the transition to turbulence (Piomelli & Zang 1991).

To alleviate these deficiencies in the case of wall-bounded flows, the Smagorinsky constant C_s is often multiplied by a damping factor depending on the wall-normal distance, the van Driest damping function being the prime example (van Driest 1956). Although the van Driest function is commonly employed, its theoretical basis has never been adequately addressed, thereby leaving it rather arbitrary. Moreover, if the determination of the distance is straightforward in the case of a plane boundary, it becomes more ambiguous near a curved boundary or a sharp corner. An approach free from the use of the wall-normal distance is therefore desirable. The dynamic SGS model intends to evaluate the Smagorinsky constant (from the resolved motions) as the calculation progresses (Germano *et al.* 1991) and thus avoids the need to specify *a priori*, or tune, the value of C_s. In brief, the adjustment of C_s relies on the Germano identity (Germano 1992) and assumes the scale similarity of the resolved velocity fluctuations at scales comparable to Δ (Meneveau & Katz 2000). This methodology yields a coefficient $C_s(\boldsymbol{x}, t)$ that varies with position and time and vanishes near the boundary with the correct behaviour (Piomelli 1993). It is beyond dispute that the dynamic procedure greatly improves the capability of the original Smagorinsky model; however, this progress is also accompanied with a certain deterioration of the numerical stability and with an increase of the computational cost. In this situation, it is legitimate to seek for an SGS model that would achieve a better compromise between accuracy and manageability: ideally, as simple as the original Smagorinsky model and as accurate as the dynamic Smagorinsky model.

2.2. *SGS modelling of anisotropic turbulent dynamics*

Turbulence near a boundary is highly anisotropic and subject to strong shear effects. The customary theoretical background for representing the unresolved small-scale dynamics should be extended. A more general approach is desirable to encompass anisotropy effects and account for the presence of the mean shear. Here, the manifestation of the mean shear should be understood in the statistical sense; it signifies, first and foremost, that the ensemble-averaged resolved rate-of-strain tensor does not reduce to zero: $|\langle \overline{S}(\boldsymbol{x}, t) \rangle| \neq 0$ (Monin & Yaglom 1975). As previously mentioned, the subgrid model should ensure the correct mean drain of energy from the grid-scale to subgrid-scale motions. In the presence of a mean shear, the energy cascade to small scales results from two different physical mechanisms associated with two distinct terms in the statistically averaged equations, namely, the nonlinear transfer term and the linear (or rapid) transfer term (Sagaut, Deck & Terracol 2006, for details). The rapid transfer term (see Craya 1958) accounts for the non-zero mean rate of strain $\langle \overline{S}(\boldsymbol{x}, t) \rangle$. It is therefore expected $\langle \overline{S}(\boldsymbol{x}, t) \rangle$ to enter into the formulation of the mean SGS energy flux, and consequently, of $\nu_T(\boldsymbol{x}, t)$. This reasoning encourages us to decompose the resolved velocity field $\overline{\boldsymbol{u}}(\boldsymbol{x}, t)$ into a (statistical) mean and a fluctuating part. This is the guideline of our work, in the continuation of previous attempts made by Schumann (1975) and Sullivan, McWilliams & Moeng (1994). However, our approach distinguishes itself from these models by connecting explicitly to the exact scale-by-scale energy budget of a (locally) homogeneous turbulent shear flow, and therefore, removing some arbitrariness in the form of $\nu_T(\boldsymbol{x}, t)$.

Including anisotropy effects in the SGS modelling has been undertaken in many different ways (Sagaut 2001, for a comprehensive description). The present approach relies on a decomposition of the resolved field $\overline{\boldsymbol{u}}(\boldsymbol{x}, t)$ into a mean (or statistically averaged) and a fluctuating part. It is informative to mention that an alternative decomposition of $\overline{\boldsymbol{u}}(\boldsymbol{x}, t)$, into a large-scale and a small-scale component, has been extensively explored. This refers to the variational multi-scale (VMS) method, which originates with the works of Temam and his colleagues on multi-level methods (Dubois, Jauberteau & Temam 1999), and has been developed by Hughes, Mazzei & Jansen (2000) and many others thereafter (Berselli, Iliescu & Layton 2005, for a review). This decomposition arises from the motivation to build an eddy-viscosity on either the small-scale or the large-scale part of $\overline{\boldsymbol{u}}(\boldsymbol{x}, t)$ and make it act on the small-scale part of the resolved motions only. When applied to the Smagorinsky model, this procedure indeed leads to a depleted SGS energy transfer compared to the original Smagorinsky model, and numerical tests are found very satisfactory for the LES of turbulent channel flows (Hughes, Oberai & Mazzei 2001). Our decomposition (into a mean and a fluctuating part) is clearly different as it is defined in a statistical sense and does not involve multi-scale components. Our main motivation was to construct a model consistent with the mean (statistical) SGS energy budget – an essential constraint for turbulence modelling – and sufficiently manageable to be of practical use for engineering flow simulations.

2.3. *Our proposal: a shear-improved eddy-viscosity*

The theoretical basis of our model was put forward by Toschi *et al.* (2000) on account of previous numerical and experimental studies on wall-bounded turbulence (Benzi *et al.* 1999; Toschi *et al.* 1999; Ruiz-Chavarria *et al.* 2000). For simplicity, we shall here recast and formulate the key arguments in the ideal case of a statistically stationary homogeneous shear flow (Monin & Yaglom 1975).

In a homogeneous shear flow, the velocity field $\boldsymbol{u}(\boldsymbol{x}, t)$ may be decomposed into $u_i(\boldsymbol{x}, t) = u_i'(\boldsymbol{x}, t) + (\partial U_i/\partial x_j)x_j$, where $U_i(\boldsymbol{x})$ and $u_i'(\boldsymbol{x}, t)$ denote the mean and fluctuating parts of the velocity, respectively. Starting from the exact dynamical equations for the two-point correlation function $R(\boldsymbol{r}) = \langle u_i'(\boldsymbol{x}, t)u_i'(\boldsymbol{x} + \boldsymbol{r}, t)\rangle$ and by integrating this equation over a sphere B_r of radius r centred at $\boldsymbol{x}$, we can establish an energy budget (at scale r) which takes the form (see Casciola *et al.* 2003; Danaila, Antonia & Burattini 2004):

$$S_3^{tr}(r) + S_3^{pr}(r) = -\tfrac{4}{3}\varepsilon r + 2\nu\frac{\mathrm{d}}{\mathrm{d}r}\left(\frac{1}{4\pi r^2}\oint_{\partial B_r}\langle|\delta\boldsymbol{u}'(\boldsymbol{x}, \boldsymbol{r}, t)|^2\rangle\,\mathrm{d}S\right). \qquad (2.1)$$

The two contributions $S_3^{tr}(r)$ and $S_3^{pr}(r)$ arise from the nonlinear term of the Navier–Stokes equations. On the right-hand side of (2.1), ε denotes the mean rate of energy dissipation and the second term encompasses finite-Reynolds-number effects (at scales larger than r) with $\delta\boldsymbol{u}'(\boldsymbol{x}, \boldsymbol{r}, t) \equiv \boldsymbol{u}'(\boldsymbol{x} + \boldsymbol{r}, t) - \boldsymbol{u}'(\boldsymbol{x}, t)$. The energy budget (2.1) is the generalization of the Kármán–Howarth equation for homogeneous shear turbulence (Hinze 1976). In the framework of LES, it may also be interpreted as the proper mean SGS energy budget with respect to the grid scale r. More explicitly,

$$S_3^{tr}(r) = \frac{1}{4\pi r^2}\oint_{\partial B_r}\left(\langle|\delta\boldsymbol{u}'(\boldsymbol{x}, \boldsymbol{r}, t)|^2\delta u_i'(\boldsymbol{x}, \boldsymbol{r}, t)\rangle + \frac{\partial U_i}{\partial x_j}r_j\langle|\delta\boldsymbol{u}'(\boldsymbol{x}, \boldsymbol{r}, t)|^2\rangle\right)\mathrm{d}S_i \qquad (2.2)$$

represents the transfer of kinetic energy from grid-scale motions (at scales larger than r) to subgrid-scale motions. Also, it indicates that this transfer results from both the grid-scale turbulent fluctuations and the mean shear. These two effects correspond, respectively, to the nonlinear triple-correlation term and the rapid (or linear) term entering into the spectral decomposition of the energy transfer, as first evidenced by Craya (1958). The second term on the left-hand side of (2.1) represents a production of SGS kinetic energy induced by the mean shear, and is expressed as

$$S_3^{pr}(r) = \frac{1}{4\pi r^2}\int_{B_r} 2\frac{\partial U_i}{\partial x_j}\langle\delta u_i'(\boldsymbol{x}, \boldsymbol{r}, t)\delta u_j'(\boldsymbol{x}, \boldsymbol{r}, t)\rangle\,\mathrm{d}V. \qquad (2.3)$$

In brief, the budget (2.1) means that SGS dynamics are sustained against molecular dissipation (represented by the right-hand side) by the transfer of energy from grid-scale motions ($S_3^{tr}(r)$) and the energy production induced directly by the mean shear ($S_3^{pr}(r)$).

As mentioned in §1, the estimate of the SGS energy flux is of prime importance in the modelling of the eddy-viscosity. In the previous budget, this flux should be identified with $S_3^{tr}(\Delta)/\Delta$. Roughly speaking, we may consider that turbulent grid-scale velocity differences, $\delta u'(\Delta)$, typically behave as the fluctuating part of the resolved rate-of-strain $|\overline{S}'|$ multiplied by Δ: $\delta u'(\Delta) \approx |\overline{S}'|\Delta$. In the same way, $\delta U(\Delta) \approx |\langle\overline{S}\rangle|\Delta$. The (exact) expression (2.2) therefore suggests that the mean SGS energy flux should involve two separate contributions of order $\Delta^2\langle|\overline{S}'|^3\rangle$ and $\Delta^2\langle|\overline{S}\rangle|\langle|\overline{S}'|^2\rangle$, respectively. Accordingly, our proposed *shear-improved eddy-viscosity* is written as

$$\nu_T(\boldsymbol{x}, t) = (C_s\Delta)^2 \cdot (|\overline{S}(\boldsymbol{x}, t)| - |\langle\overline{S}(\boldsymbol{x}, t)\rangle|), \qquad (2.4)$$

where the angle brackets $\langle\ \rangle$ *a priori* denote an ensemble average, which, in practice, is a space average over homogeneous directions and/or a time average (this specific issue will be mentioned again in §4). From our definition (2.4), the modelled mean SGS energy flux is

$$F_{sgs} \equiv -\langle\tau_{ij}\overline{S}_{ij}\rangle = (C_s\Delta)^2 \,(\langle|\overline{S}|^3\rangle - |\langle\overline{S}\rangle|\langle|\overline{S}|^2\rangle). \qquad (2.5)$$

Straightforwardly, this flux vanishes if the resolved turbulence disappears, i.e. if $\overline{S} = \langle\overline{S}\rangle$. We shall now argue that it is also consistent (to some extent) with the previous estimation of the mean SGS energy flux in a homogeneous turbulent shear flow.

In flow regions where $|\overline{S'}| \gg |\langle\overline{S}\rangle|$, the SGS energy flux is expected to reduce to the contribution of order $\Delta^2\langle|\overline{S'}|^3\rangle$. In these regions, the mean shear is too weak to perturb the grid-scale dynamics; eddies of size comparable to the grid-scale Δ adjust dynamically via nonlinear interactions to transfer energy to SGS motions. This is the standard mechanism behind homogeneous and isotropic turbulence (Frisch 1995). From our expression (2.5), we remark that the Smagorinsky estimate $F_{sgs} \simeq (C_s\Delta)^2\langle|\overline{S'}|^3\rangle$ is consistently recovered in that case. In regions where $|\langle\overline{S}\rangle| \gg |\overline{S'}|$, the behaviour of the flow is clearly different. Eddies of size comparable to the grid-scale have no time to adjust dynamically and are rapidly distorted by the mean shear (Liu, Katz & Meneveau 1999). In these regions, the SGS energy flux is driven by the mean shear and therefore is dominated by the contribution of order $\Delta^2|\langle\overline{S}\rangle||\overline{S'}|^2\rangle$. From (2.5) and assuming that $\langle|\overline{S}|^3\rangle \approx \langle|\overline{S}|^2\rangle^{3/2}$, we obtain $F_{sgs} \simeq 1/2 \ (C_s\Delta)^2|\langle\overline{S}\rangle| \ \langle|\overline{S'}|^2\rangle$ in agreement with the previous reasoning. We may thus conclude that our proposal (2.4) for the eddy-viscosity is consistent with the SGS energy budget of (locally homogeneous) shear turbulence in the two limiting situations $|\overline{S'}| \gg |\langle\overline{S}\rangle|$ and $|\langle\overline{S}\rangle| \gg |\overline{S'}|$. The first results concerning plane-channel flows (see §3) indicate that the proposed model actually bridges these two situations without the need for additional adjustment.

The formulation of our SGS model exhibits similarities with the model originally introduced by Schumann (1975) which relies on a two-part eddy-viscosity accounting for the interplay between the nonlinear energy cascade present in isotropic turbulence and mean shear effects associated with anisotropy. However, our model clearly differs from Schumann's proposal, which requires an empirical prescription for the 'inhomogeneous eddy-viscosity'. An important point is that our model cannot be obtained by simplifying Schumann's formulation. Indeed, the key element of our study is that the relevant contribution to the SGS energy flux near the wall must behave as $|\langle\overline{S}\rangle| \ \langle|\overline{S'}|^2\rangle$. By making the mean-shear-based eddy-viscosity act on the mean shear itself, Schumann's proposal dispenses with the necessity for this correct behaviour. Also, the simple formulation $\nu_T = (C_s\Delta)^2|\overline{S} - \langle\overline{S}\rangle|$ (Berselli *et al.* 2005) leads to $F_{sgs} \simeq (C_s\Delta)^2|\langle\overline{S}\rangle|^2\langle|\overline{S'}|\rangle$ when $|\langle\overline{S}\rangle| \gg |\overline{S'}|$, which contradicts the expression of the mean SGS energy flux.

3. LES of turbulent plane-channel flows

Over the last twenty years, LES of wall-bounded flows have received considerable attention (Piomelli & Balaras 2002, for a review), with the turbulent plane-channel flow (Kim, Moin & Moser 1987) being the prototypical case. This flow allows for the investigation of shear effects in a simple geometry and has therefore provided a useful test bed of our eddy-viscosity model. Furthermore, we have been able to confront our results on mean velocity, turbulence intensities and Reynolds stress profiles with the well-established literature present on that case, e.g. the comprehensive DNS database obtained by Moser, Kim & Mansour (1999) or Hoyas & Jimenez (2006).

3.1. *Numerical simulations*

We performed two LES at $Re_\tau = 395$ and $Re_\tau = 590$, where Re_τ is the Reynolds number based on the friction velocity u_τ: $Re_\tau \equiv u_\tau H/\nu$ (H is the half width of the channel). These two cases correspond to the DNS conducted by Moser *et al.* (1999).
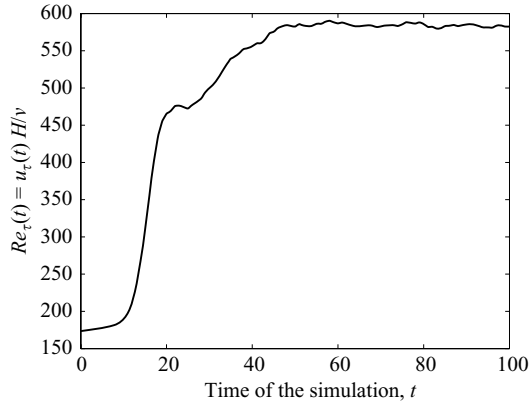
FIGURE 1. The time development of the Reynolds number $Re_\tau(t)$ based on the plane-averaged friction velocity $u_\tau(t)$. Asymptotic mean $Re_\tau = 590$.

Periodic boundary conditions were imposed in the streamwise and spanwise directions; no-slip conditions at the wall. The flow was simulated by integrating the filtered Navier–Stokes equations (1.1) with the prescribed eddy-viscosity (2.4). The right-hand side of (1.1) was supplemented by an external pressure-gradient $\Delta p_{ext}/4\pi H$ in order to drive the flow in the streamwise direction. The pressure difference $\Delta p_{ext}(t)$ was adjusted dynamically to keep a constant flow rate through the channel. The integration relied on a Fourier–Chebyshev pseudospectral solver (de-aliased by using the 3/2 rule) based on a third-order Runge–Kutta scheme. A pseudospectral method has been used to limit (numerical) discretization errors and therefore concentrate on modelling errors. More details about the numerical code can be found in Xu, Zhang & Nieuwstadt (1996). To prevent numerical instability, the overall viscosity $\nu + \nu_T$ was clipped to zero whenever negative. In practice, this clipping never operated because negative values of ν_T (occurring mainly in the viscous sublayer) were always much smaller (in amplitude) than ν. The Smagorinsky constant was fixed to its standard value $C_s = 0.16$ (for homogeneous and isotropic turbulence) and the scale Δ was estimated as $(\Delta x \Delta y \Delta z)^{1/3}$ (Deardorff 1970), where Δx, Δy and Δz denote the local grid spacings in each direction. In the following, the grid-scale velocity components are $U + u'$, v' and w' along the streamwise, wall-normal and spanwise directions, respectively.

3.2. *Numerical results*

At initial time, velocity distributions were designed to satisfy a Poiseuille profile plus a small random perturbation. The time development of $Re_\tau(t) = u_\tau(t)H/\nu$, where $u_\tau(t)$ is expressed as the square root of the plane-averaged wall shear stress, is plotted in figure 1 for $Re_\tau = 590$. A transition (drag crisis) to the appropriate turbulent regime occurs naturally as the integration (with the eddy-viscosity (2.4)) progresses. This feature constitutes a first improvement over the Smagorinsky model, for which such transition is not captured. Once a developed turbulent state was achieved, statistics were accumulated.

The mean velocity $U^+(y^+)$ is displayed as a function of the wall-normal distance y^+ in figure 2. From now on, the average is used in time and over horizontal planes (homogeneous directions). Mean velocity profiles agree well with the DNS reference data obtained by Moser *et al.* (1999) for both Reynolds numbers considered. The comparison with the dynamic Smagorinsky model is also satisfactory (Piomelli 1993).
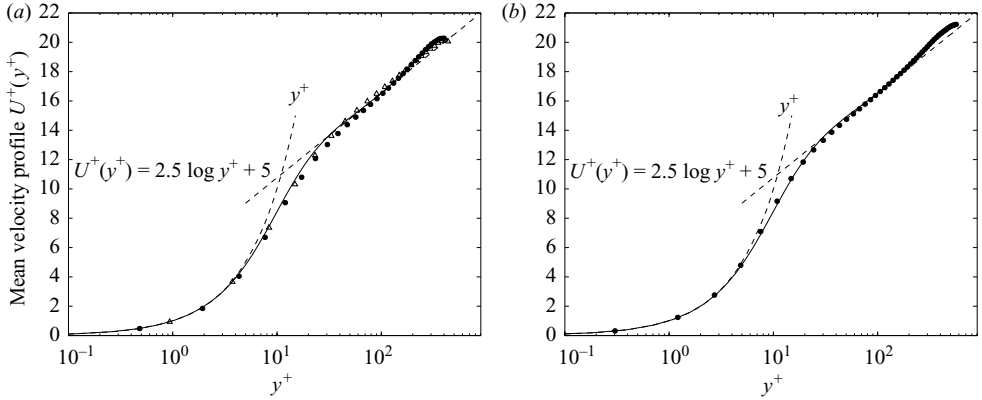
FIGURE 2. (*a*) (●) mean-velocity profile (in wall units) at $Re_\tau = 395$. The computational domain (in outer units) is $4\pi H \times 2H \times 2\pi H$ with $64 \times 65 \times 64$ grid points. In comparison with (−) the DNS data obtained by Moser *et al.* (1999) in the domain $2\pi H \times 2H \times \pi H$ with $256 \times 193 \times 192$ grid points, and (△) a computation of the dynamic Smagorinsky model carried out by Piomelli (personal communication) in the domain $5\pi H/2 \times 2H \times \pi H/2$ with $48 \times 49 \times 48$ grid points (using a pseudospectral solver). (*b*) (●) mean-velocity profile at $Re_\tau = 590$ with $96 \times 97 \times 96$ grid points. In comparison with (−) the DNS data with $384 \times 257 \times 384$ grid points.
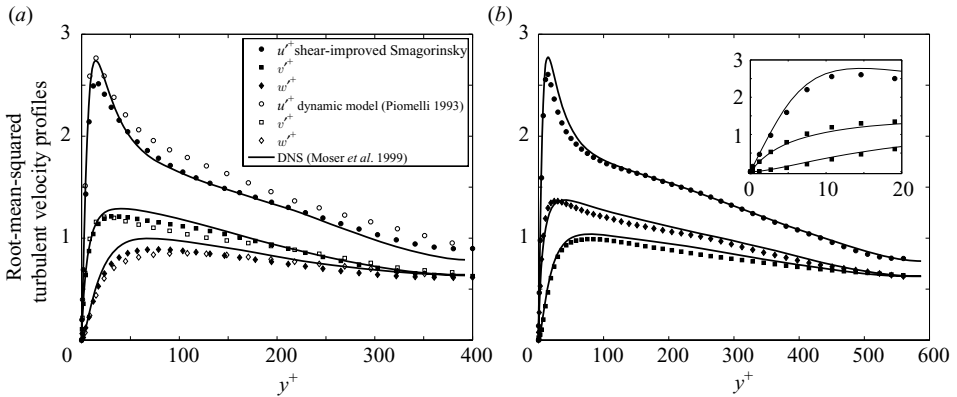

FIGURE 3. (*a*) Turbulent intensity profiles at $Re_\tau = 395$ in comparison with DNS data and LES data obtained with the dynamic Smagorinsky model. (*b*) Turbulent intensity profiles at $Re_\tau = 590$. The inset focuses on near-wall behaviour in comparison with DNS data.

Turbulence intensity profiles (normalized by the squared friction velocity) are shown in figure 3. Also here, the profiles compare very well with the DNS data and LES results based on the dynamic Smagorinsky model; the positions of the peaks are captured well and the errors on the peak values remain acceptable (the peak of u^+ is off by 10 %). As for the dynamic Smagorinsky model, a slight drop is observed in the log-layer for the spanwise and wall-normal components. On the contrary, the streamwise component fits the DNS data well. In the proximity of the wall, the correct behaviour is obtained.

These positive results presumably indicate that our eddy-viscosity has captured the essential shear effects in wall-bounded turbulence. In order to check this, the ratio $\sqrt{\langle |S'|^2 \rangle}/|\langle S \rangle|$ is shown as a function of y^+ in figure 4. For $y^+ \lesssim 25$, the mean shear dominates over the fluctuating part of the rate-of-strain, indicating
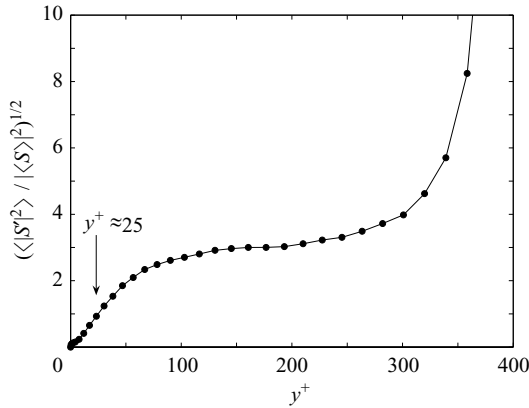
FIGURE 4. The ratio $\sqrt{\langle|S'|^2\rangle}/|\langle S \rangle|$ is displayed as a function of the wall-normal distance y^+ in the LES at $Re_\tau = 395$. For $y^+ \lesssim 25$, the mean shear dominates over the fluctuating part of rate-of-strain. In that region, our eddy-viscosity differs from the original Smagorinsky model.
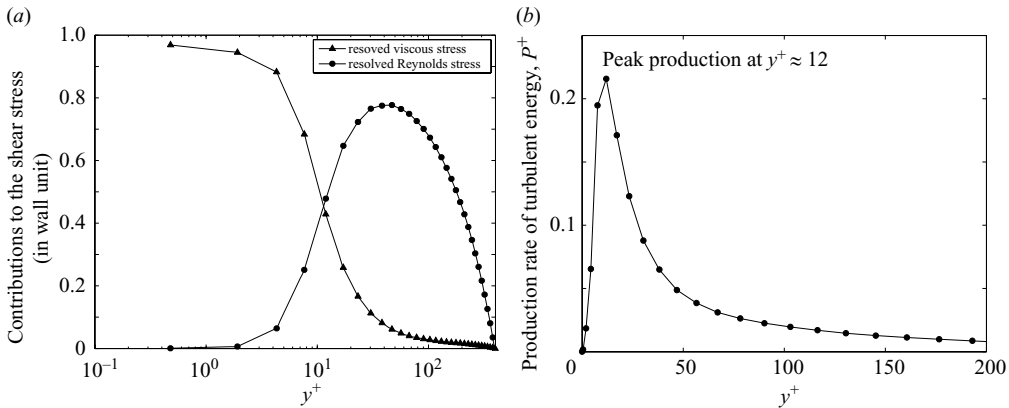

FIGURE 5. (*a*) The viscous and Reynolds stresses (computed from the resolved velocity) at $Re_\tau = 395$. The two contributions are equal at $y^+ \approx 12$, in full agreement with DNS results. (*b*) The peak production of turbulent energy also occurs at $y^+ \approx 12$, as expected.

the predominance of the mean-shear component of the eddy-viscosity in that region. Note that the transition distance $y^+ \simeq 25$ is fully consistent with the empirical distance $A^+ = 25$ commonly used in the van Driest damping function (Pope 2000). In the log-layer, $\sqrt{\langle|S'|^2\rangle}/|\langle S \rangle|$ increases slowly with y^+ (the standard description of the log-layer predicts a linear increase resulting from $|\langle S \rangle| \propto 1/y$ and $\langle|S'|^2\rangle \propto u_\tau^2/\Delta^2$) and eventually diverges around the centreline of the channel. Thus, we may claim that our model suitably bridges the situation where the mean shear prevails (close to the boundaries) and the situation where the fluctuating part of the rate-of-strain dominates (in the bulk of the channel).

The viscous, dU^+/dy^+, and the Reynolds, $-\langle u'^+ v'^+ \rangle$, contributions to the resolved stress are shown in figure 5. They are equal for $y^+ \approx 12$, in perfect agreement with DNS results (Pope 2000). The peak value of the turbulent energy production, $-\langle u'^+ v'^+ \rangle \, dU^+/dy^+$, occurs at the same distance $y^+ \approx 12$, as expected from the Navier–Stokes equations. The grid-scale Reynolds stress profiles are shown in
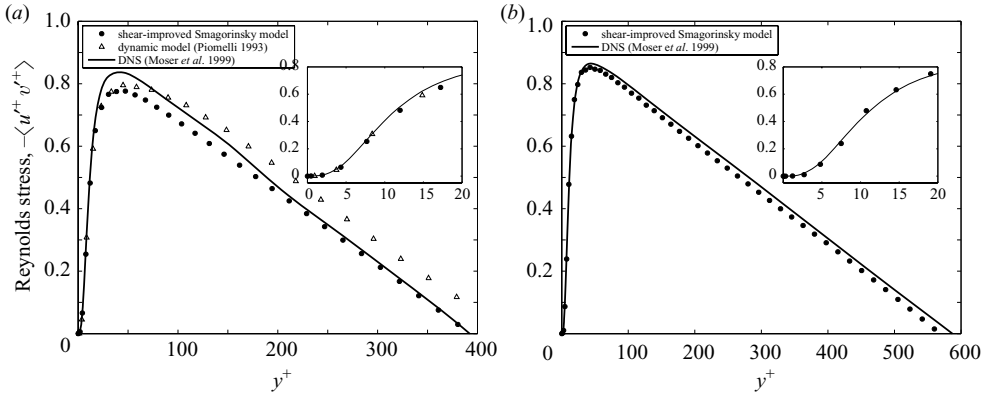
FIGURE 6. (*a*) Reynolds stress at $Re_\tau = 395$ (computed from the resolved velocity). (*b*) The Reynolds stress at $Re_\tau = 590$. The insets focus on the near-wall behaviour.

figure 6. The agreement with the DNS and the LES based on the dynamic Smagorinsky model is fair and also the behaviour close to the wall is satisfactory.

4. Discussions and perspectives

We have presented a very simple SGS model consisting in a physically sound improvement over the well-established Smagorinsky model, in connection with the exact scale-by-scale energy budget of homogeneous shear turbulence. Our first results for turbulent plane-channel flows indicate that the proposed model possesses a very good predictive capability (essentially equivalent to the dynamic Smagorinsky model) with a computational cost and a manageability comparable to the original Smagorinsky model; this was our main goal.

The generalization to more complex non-homogeneous flows is *a priori* straightforward since no geometrical argument enters into the definition of the eddy-viscosity. However, an appropriate average must be specified in the absence of homogeneity directions. As a natural candidate, we suggest an average in time to evaluate the mean components of the rate-of-strain tensor (if the flow is statistically stationary). In the case of non-stationary flows, an ensemble average (over several realizations) may be envisaged. These points are the subject of current investigations. A deeper analysis of the model in the framework of the rapid-slow decomposition introduced by Shao, Sarkar & Pantano (1999) will also be carried out.

REFERENCES

BENZI, R., AMATI, G., CASCIOLA, C., TOSCHI, F. & PIVA, R. 1999 Intermittency and scaling laws for wall bounded turbulence. *Phys. Fluids* **11** (6), 1284–1286.

BERSELLI, L. C., ILIESCU, T. & LAYTON, W. J. 2005 *Mathematics of Large Eddy Simulation of Turbulent Flows*. Springer.

CASCIOLA, C. M., GUALTIERI, P., BENZI, R. & PIVA, R. 2003 Scale-by-scale budget and similarity laws for shear turbulence. *J. Fluid Mech.* **176**, 105–114.

CRAYA, A. 1958 Contribution à l'analyse de la turbulence associée à des vitesses moyennes. *P. S. T. Ministère de l'Air* **345**.

DANAILA, L., ANTONIA, R. & BURATTINI, P. 2004 Progress in studying small-scale turbulence using exact two-point equations. *New J. Phys.* **6**, 128.

DEARDORFF, J. W. 1970 A numerical study of three-dimensional turbulent channel flow at large Reynolds numbers. *J. Fluid Mech.* **41**, 453.

VAN DRIEST, E. R. 1956 On turbulent flow near a wall. *J. Aero. Sci.* **23**, 1007–1011.

DUBOIS, T., JAUBERTEAU, F. & TEMAM, R. 1999 *Dynamic Multilevel Methods and the Numerical Simulation of Turbulence*. Cambridge University Press.

FRISCH, U. 1995 *Turbulence: The Legacy of A. N. Kolmogorov*. Cambridge University Press.

GERMANO, M. 1992 Turbulence: the filtering approach. *J. Fluid Mech.* **238**, 325–336.

GERMANO, M., PIOMELLI, U., MOIN, P. & CABOT, W. H. 1991 A dynamic subgrid-scale eddy viscosity model. *Phys. Fluids* A **3**, 1760.

GHOSAL, S. & MOIN, P. 1995 The basic equations for the large eddy simulation of turbulent flows in complex geometry. *J. Comput. Phys.* **118**, 24–37.

HINZE, J. O. 1976 *Turbulence*. McGraw–Hill.

HOYAS, S. & JIMENEZ, J. 2006 Scaling of velocity fluctuations in turbulent channels up to $Re_\tau = 2000$. *Phys. Fluids* **18**, 011702, http://torroja.dmt.upm.es/ftp/channels/data/.

HUGHES, T. J. R., MAZZEI, L. & JANSEN, K. E. 2000 Large eddy simulation and the variational multiscale method. *Compu. Visualiz. Sci.* **3**, 47.

HUGHES, T. J. R., OBERAI, A. & MAZZEI, L. 2001 Large eddy simulation of turbulent channel flows by the variational multiscale method. *Phys. Fluids* **13** (6), 1784–1799.

KIM, J., MOIN, P. & MOSER, R. D. 1987 Turbulent statistics in fully developed channel flow at low Reynolds number. *J. Fluid Mech.* **177**, 133.

KRAICHNAN, R. H. 1976 Eddy-viscosity in two and three dimensions. *J. Atmos. Sci.* **33**, 1521–1536.

LEONARD, A. 1974 Energy cascade in large-eddy simulations of turbulent fluid flows. *Adv. Geophys.* A **18**, 237–248.

LESIEUR, M. 1997 *Turbulence in Fluids*, 3rd edn. Kluwer.

LESIEUR, M. & METAIS, O. 1996 New trends in large-eddy simulations of turbulence. *Annu. Rev. Fluid. Mech.* **28**, 45–82.

LILLY, D. K. 1967 The representation of small-scale turbulence in numerical simulation experiments. In *Proc. IBM Sci. Comput. Symp. Environ. Sci*, p. 195.

LIU, S., KATZ, J. & MENEVEAU, C. 1999 Evolution and modelling of subgrid scales during rapid straining of turbulence. *J. Fluid Mech.* **387**, 281–320.

MENEVEAU, C. & KATZ, J. 2000 Scale-invariance and turbulence models for large-eddy simulation. *Annu. Rev. Fluid Mech.* **32**, 1–32.

MOIN, P. & KIM, J. 1982 Numerical investigation of turbulent channel flow. *J. Fluid Mech.* **118**, 341–377.

MONIN, A. S. & YAGLOM, A. M. 1975 *Statistical Fluid Mechanics*. MIT Press, Cambridge MA.

MOSER, R. D., KIM, J. & MANSOUR, N. N. 1999 Direct numerical simulation of turbulent channel flow up to $Re_\tau = 590$. *Phys. Fluids* **11** (4), 943–945, http://www.tam.uiuc.edu/Faculty/Moser.

PEROT, B. & MOIN, P. 1995 Shear-free turbulent boundary layers. Part 1. Physical insights into near wall turbulence. *J. Fluid Mech.* **295**, 199–227.

PIOMELLI, U. 1993 High Reynolds number calculations using the dynamic subgrid-scale stress model. *Phys. Fluids* A **5** (6), 1484.

PIOMELLI, U. 1999 Large-eddy simulation: achievements and challenges. *Prog. Aerosp. Sci.* **35**, 335–362.

PIOMELLI, U. & BALARAS, E. 2002 Wall-layer models for large-eddy simulations. *Annu. Rev. Fluid Mech.* **34**, 349–374.

PIOMELLI, U. & ZANG, T. A. 1991 Large-eddy simulation of transitional channel flow. *Comput. Phys. Commun.* **65**, 224–230.

POPE, S. B. 2000 *Turbulent Flows*. Cambridge University Press.

ROGALLO, R. S. & MOIN, P. 1984 Numerical simulation of turbulent flows. *Annu. Rev. Fluid Mech.* **16**, 99–137.

RUIZ-CHAVARRIA, G., CILIBERTO, S., BAUDET, C. & LÉVÊQUE, E. 2000 Scaling properties of the streamwise component of velocity in a turbulent boundary layer. *Physica* D **141**, 183–198.

SAGAUT, P. 2001 *Large Eddy Simulation for Incompressible Flows*. Springer.

SAGAUT, P., DECK, S. & TERRACOL, M. 2006 *Multiscale and Multiresolution Approaches in Turbulence*. Imperial College Press.

SCHUMANN, U. 1975 Subgrid scale model for finite difference simulations of turbulent flows in plane channels and annulli. *J. Comput. Phys.* **18**, 376–404.

SHAO, L., SARKAR, S. & PANTANO, C. 1999 On the relationship between the mean flow and subgrid stresses in large eddy simulation of turbulent shear flows. *Phys. Fluids* **11** (5), 1229–1248.

SMAGORINSKY, J. 1963 General circulation experiments with the primitive equations. 1. The basic experiment. *Mon. Weather Rev.* **91**, 99.

SULLIVAN, P., McWILLIAMS, J. C. & MOENG, C.-H. 1994 A subgrid-scale model for large-eddy simulation of planetary boundary-layer flows. *Boundary-Layer Met.* **71**, 247–276.

TOSCHI, F., AMATI, G., SUCCI, S., BENZI, R. & PIVA, R. 1999 Intermittency and structure functions in channel flow turbulence. *Phys. Rev. Lett.* **82**, 5044–5047.

TOSCHI, F., LÉVÊQUE, E. & RUIZ-CHAVARRIA, G. 2000 Shear effects in nonhomogeneous turbulence. *Phys. Rev. Lett.* **85**, 1436.

XU, C. X., ZHANG, Z. & NIEUWSTADT, F. M. 1996 Origin of high kurtosis in viscous sublayer. *Phys. Fluids* **85**, 1938.